

Effect of spontaneous emission on the shortcut to adiabaticity in three-state systemsX. Shi ^{1,2} and H. Q. Zhao^{1,2,*}¹*Center of Quantum Information Technology, Chongqing Institute of Green and Intelligent Technology, Chinese Academy of Sciences, Chongqing 400714, China*²*College of Artificial Intelligence, Chongqing School, University of Chinese Academy of Sciences, Chongqing 400714, China*

(Received 27 April 2021; revised 9 October 2021; accepted 9 November 2021; published 24 November 2021)

The shortcut to adiabaticity (STA) is a powerful technique to speed up population transfer via quantum coherent control. This paper demonstrates that STA provides a fast, robust, and efficient population transfer compared to the stimulated Raman adiabatic passage. In the ideal situation of a closed system, STA is insensitive to the detunings and Rabi frequencies, and the undesired diabatic transitions could be eliminated by the auxiliary pulses, so the complete population transfer from the initial state to the target state in the designed adiabatic passage can be rapidly achieved against the inevitable amplitude noises of the interactions and systematic errors. When we consider the situation including the environment noises, spontaneous emission from the intermediate state $|2\rangle$ in STA can be sufficiently ignored in the cases of the dark-state evolution and quantum overdamping, since the state $|2\rangle$ is thoroughly separated from the three-state system. Moreover, the diabatic transitions induced by the spontaneous emission are also sufficiently suppressed in STA.

DOI: [10.1103/PhysRevA.104.052221](https://doi.org/10.1103/PhysRevA.104.052221)**I. INTRODUCTION**

In the last ten years, a technique named the shortcut to adiabaticity (STA) has found widespread applications in atomic, molecular, and solid-state physics for preparing and driving internal and motional states with high fidelity [1]. In general, there are two well-known approaches to achieve state preparation or population transfer. One is making use of resonant pulses and the other is based on adiabatic approaches [2]. Resonant pulses with an area π for the Rabi frequency may be fast for the population transfer, but sensitive and nonrobust to the amplitude noises of the interactions and systematic errors. On the other hand, adiabatic approaches are robust but slow [3]. STA, portrayed artistically and informally as a turtle on wheels [1], possesses both the advantages of resonant pulses and adiabatic approaches. It reaches the same final conditions of a slow adiabatic process in a shorter time and is robust against the fluctuations of the controlling pulses [4,5].

Different strategies for STA have been developed and applied, such as counterdiabatic driving [6–9], invariant-based inverse engineering [10,11], the streamlined fast-forward approach [12], variational methods [13–15], and so on [16–21]. Some of the basic STA techniques are related to each other, and can be made potentially equivalent by properly adjusting the reference Hamiltonian, e.g., counterdiabatic driving and invariant-based inverse engineering [22]. For simplicity, we consider the original method of counterdiabatic driving that the expression STA is coined [6]. The key idea of STA is to find a driving Hamiltonian $\hat{H}(t)$ to exactly evolve the system along a selected instantaneous eigenstate $|\lambda_n\rangle$ of the initial Hamiltonian \hat{H}_0 .

As a powerful and universal technique, STA is available for most physical platforms to accelerate state preparations and fighting decoherence [23–26]. It has been theoretically designed in many solid quantum systems (e.g., optical waveguides [27,28], superconducting circuits [29], quantum dots [30], and trapped ions [31,32]), for fast and robust population transfer in quantum gate manipulation [33,34], entanglement generation [35], single photon production [36], and so on. Experimental achievements of this technique have also been reported including acceleration of Bose-Einstein condensates in optical lattices [37], rapid control of electron spins in the nitrogen-vacancy center in diamond [38,39], fast quantum state transfer in cold atoms [40], implementation of a shortcut to the adiabatic transport of a trapped ion in phase space [41], and the speedup of the adiabatic population transfer in superconducting circuits [42,43].

Although theoretical and experimental researches demonstrate that STA is an optimal approach for population manipulation, the transfer efficiencies observed in experiments leave a lot to be desired. There is no doubt that a perfect 100% transfer efficiency could be achieved in a closed quantum system. However, the population losses induced by the noises are inevitable in practice, since quantum systems are always exposed to various decoherent effects. Previous work has demonstrated that STA is robust versus different perturbations in two-state systems. The main error sources are the deviations in the coupling terms, such as fluctuations in the laser intensities or inaccurate realizations of the ideal functions [2,6]. All these losses come from the amplitude noises of the interactions and systematic errors. The quantum losses, coming from the interaction between a quantum system and its environment (such as dephasing and spontaneous emission within and outside of a system), are rarely considered in STA. Recently, the dephasing effects on STA have been studied

*hqzhao@cigit.ac.cn

in two- and three-state systems [44,45], but the effects of spontaneous emission on STA have never been discussed. Generally, spontaneous emission outside of a quantum system is always treated easily by a non-Hermitian Hamiltonian in the resonant pulses and adiabatic approaches [46–50]. One can use the Schrödinger equation and model the losses by adding an imaginary decay rate in the Hamiltonian corresponding to the excited state. However, the spontaneous emission within a system may be modeled in a more sophisticated fashion, since a complicated density matrix for the Liouville equation is required. In this paper, we concentrate on the effects of spontaneous emission within a three-state system. The population transfer in a three-state system is basically achieved by the stimulated Raman adiabatic passage (STIRAP) [51]. As an adiabatic approach, STIRAP is often sped up with STA in different strategies. Our model specially focuses on the spontaneous emission in the case of counterdiabatic STA, and can be also applied to the other strategies.

This paper is organized as follows. In Sec. II, population transfer via STA in a three-state system is constructed. Compared with STIRAP, the characteristics of STA are presented in the dark- and bright-state evolutions. In Sec. III, the effects of spontaneous emission from the intermediate state |2⟩ on STA are discussed with the Liouville equation. Finally, a summary is forwarded in Sec. IV.

II. THE MODEL IN THREE-STATE QUANTUM SYSTEMS

In three-state quantum systems, a popular and powerful technique for population transfer is STIRAP. In this technique, complete population transfer between the two end states |1⟩ and |3⟩ is realized adiabatically through an intermediate state |2⟩ by two pulses, pump and Stokes. In the most common Λ linkage pattern, states |1⟩ and |3⟩ are ground or metastable electronic levels, and the intermediate state |2⟩ is a decaying and excited electronic level. The initial state |1⟩ and the final state |3⟩ have to be on two-photon resonance; the intermediate state |2⟩ can be off resonant by a certain detuning Δ . In this situation, the evolution passage of the population transfer is guaranteed to be in one of the eigenstates of the Hamiltonian \hat{H}_0 under the adiabaticity condition. As the pulses are ordered counterintuitively, the Stokes before the pump, population transfer is adiabatically trapped in a dark adiabatic passage. This passage is a time-dependent superposition of states |1⟩ and |3⟩, and does not involve the intermediate state |2⟩. In the intuitive pulse order, the pump pulse comes first; the population transfer goes along a bright adiabatic passage which is related to the intermediate state |2⟩. Here, we should emphasize that both the dark- and bright-state evolutions are slow progresses.

To speed up the population transfer, auxiliary pulses are applied to STIRAP for achieving STA. Figure 1 shows the differences of the pulse couplings between the two approaches. The Hamiltonian of the three-state Λ system, in the rotating-wave approximation, has the form ($\hbar = 1$)

$$\hat{H} = \begin{pmatrix} 0 & \Omega_p & 0 \\ \Omega_p & \Delta & \Omega_s \\ 0 & \Omega_s & 0 \end{pmatrix} + i \begin{pmatrix} 0 & \Omega_a & \Omega_c \\ -\Omega_a & 0 & -\Omega_b \\ -\Omega_c & \Omega_b & 0 \end{pmatrix}. \quad (1)$$

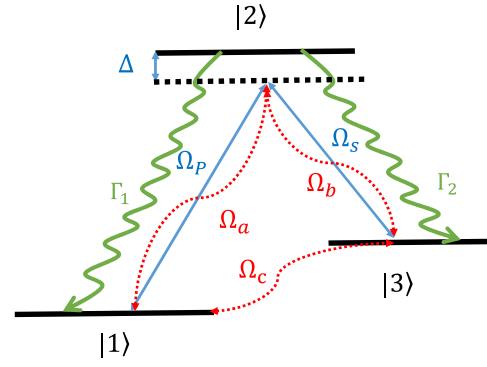


FIG. 1. Schematic of the three-state Λ system. The initial state |1⟩ and the final state |3⟩ are on two-photon resonance. The intermediate state |2⟩ is off resonant by a detuning $\Delta(t)$. The relative spontaneous emission for each pair of states is depicted by the green wavy line. The STIRAP coupling scheme is realized by the pump $\Omega_p(t)$ and Stokes $\Omega_s(t)$ pulses, and the auxiliary pulses $\Omega_a(t)$, $\Omega_b(t)$, and $\Omega_c(t)$ depicted by the dotted red lines are designed for STA.

Here the functions Ω_p and Ω_s represent Rabi frequencies of pump and Stokes pulses, and Δ is the detuning. The evolution passages for population transfer related to this Hamiltonian are defined by the adiabatic states which are time-dependent superpositions of the bare (unperturbed) states |1⟩, |2⟩, and |3⟩:

$$\begin{aligned} |\lambda_+\rangle &= \sin\theta \sin\phi |1\rangle + \cos\phi |2\rangle + \cos\theta \sin\phi |3\rangle, \\ |\lambda_0\rangle &= \cos\theta |1\rangle - \sin\theta |3\rangle, \\ |\lambda_-\rangle &= \sin\theta \cos\phi |1\rangle - \sin\phi |2\rangle + \cos\theta \cos\phi |3\rangle, \end{aligned} \quad (2)$$

with the relevant eigenvalues $\lambda_+ = \Omega \cot\phi$, $\lambda_0 = 0$, and $\lambda_- = -\Omega \tan\phi$. The time-dependent mixing angles θ and ϕ are defined by $\tan\theta = \Omega_p/\Omega_s$, $\tan 2\phi = 2\Omega/\Delta$, $\Omega = \sqrt{\Omega_p^2 + \Omega_s^2}$. The auxiliary pulses $\Omega_a(t)$, $\Omega_b(t)$, and $\Omega_c(t)$ for STA are determined by the counterdiabatic driving Hamiltonian $\hat{H}_{cd} = \sum_{n=+,-,0} |\partial_t \lambda_n(t)\rangle \langle \lambda_n(t)|$, and have the form $\Omega_a(t) = \dot{\phi} \sin\theta$, $\Omega_b(t) = \dot{\phi} \cos\theta$, $\Omega_c(t) = \dot{\theta}$ with

$$\begin{aligned} \dot{\theta} &= \frac{[\dot{\Omega}_p \Omega_s - \dot{\Omega}_s \Omega_p]}{\Omega^2}, \\ \dot{\phi} &= \frac{\{[\dot{\Omega}_p(t) \Omega_p(t) + \Omega_s(t) \dot{\Omega}_s(t)] \Delta(t)\}}{[\Omega(\Delta^2(t) + 4\Omega^2)]}. \end{aligned} \quad (3)$$

The overdot denotes a time derivative. The wave functions of this three-state system are governed by the time-dependent Schrödinger equation

$$i \begin{pmatrix} \dot{c}_1 \\ \dot{c}_2 \\ \dot{c}_3 \end{pmatrix} = \begin{pmatrix} 0 & \Omega_p + i\Omega_a & i\Omega_c \\ \Omega_p - i\Omega_a & \Delta & \Omega_s - i\Omega_b \\ -i\Omega_c & \Omega_s + i\Omega_b & 0 \end{pmatrix} \begin{pmatrix} c_1 \\ c_2 \\ c_3 \end{pmatrix}. \quad (4)$$

We assume that the system is initially in its ground state |1⟩, $c_1(-\infty) = 1$, $c_2(-\infty) = 0$, $c_3(-\infty) = 0$, and we are interested in the populations $\rho_{nn} = |c_n(+\infty)|^2$ ($n = 1, 2, 3$) at time $t \rightarrow +\infty$. In the adiabatic representation $|\lambda_+\rangle$, $|\lambda_0\rangle$,

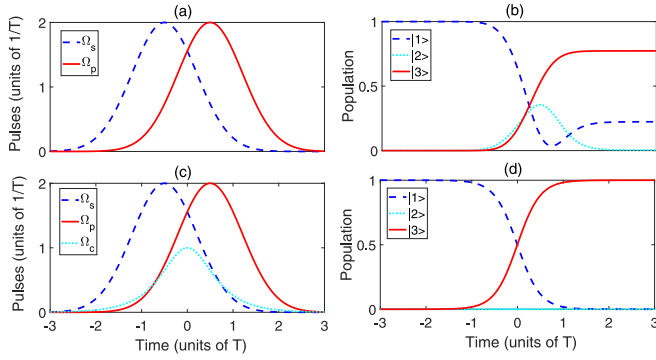


FIG. 2. Population transfer in the counterintuitive pulse sequence along the dark adiabatic passage $|\lambda_0\rangle$ for the detuning $\Delta = 2\pi \times 0.1$ MHz. (a) Pulse shapes for STIRAP. (b) Population evolution for STIRAP. (c) Pulse shapes for STA. and (d) Population evolution for STA. The Gaussian pulses are given with parameters $\Omega_0 = 2/T$, $\tau_s = -0.5T$, and $\tau_p = 0.5T$.

and $|\lambda_- \rangle$, Eq. (4) becomes

$$i \begin{pmatrix} \dot{a}_+ \\ \dot{a}_0 \\ \dot{a}_- \end{pmatrix} = \begin{pmatrix} \Omega \cot \phi & 0 & 0 \\ 0 & 0 & 0 \\ 0 & 0 & -\Omega \tan \phi \end{pmatrix} \begin{pmatrix} a_+ \\ a_0 \\ a_- \end{pmatrix}, \quad (5)$$

where a_+ , a_0 , and a_- are the probability amplitudes of the adiabatic passages. Absolutely, the diabatic transitions among the adiabatic passages are completely eliminated by the auxiliary pulses. As the system is initially prepared in one of the adiabatic passages, the population evolution will be continuously held in the corresponding passage.

To numerically compare the two approaches, STA and STIRAP, we consider the following Gaussian pulses,

$$\Omega_p(t) = \Omega_0 e^{-\frac{(t-\tau_p)^2}{T^2}}, \quad \Omega_s(t) = \Omega_0 e^{-\frac{(t-\tau_s)^2}{T^2}}, \quad (6)$$

as an example. Here, Ω_0 is the peak Rabi frequency, T is the characteristic width, and τ_p and τ_s are the pulse delay times. With these pulses, the mixed angles θ and ϕ could be confirmed and the adiabatic passage for the system evolution could be selected. Our task is to sufficiently and effectively drive the population from the ground state $|1\rangle$ to the target state $|3\rangle$.

In the counterintuitive sequence, the angle θ is initially to be zero, and then to be $\pi/2$ at the end of the population transfer. The population is carried by the dark adiabatic passage $|\lambda_0\rangle$ in STIRAP. In the adiabaticity condition, the couplings between the adiabatic passages are fairly weak such that the diabatic transitions among the adiabatic passages can be sufficiently neglected and the population could be always held in the adiabatic passage $|\lambda_0\rangle$. If the diabatic transitions exist in the excitation, the transfer efficiency could be cut down, and the population may even return to the initial state. As the pulses presented in Fig. 2, the adiabaticity condition is destroyed by the pulse intensities. In STIRAP, the final population of the target state $|3\rangle$ is only 77.3% owing to the diabatic transitions depicted in Fig. 2(b). As the auxiliary pulse Ω_c is applied to achieve the proposal of STA, the diabatic transitions are completely eliminated, and the transfer efficiency is enhanced up to the expected value of 100% in

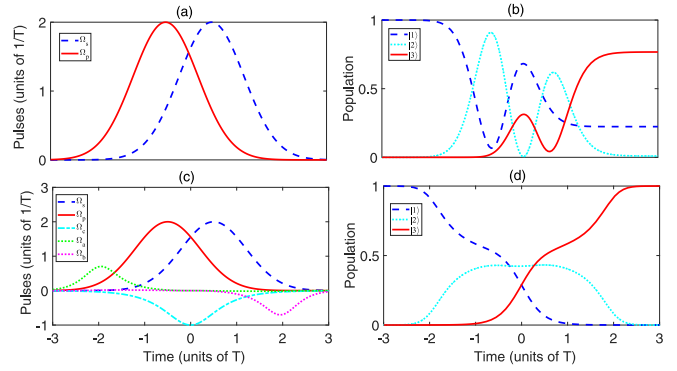


FIG. 3. Population transfer in the intuitive pulse sequence along the bright adiabatic passage $|\lambda_- \rangle$ for the detuning $\Delta = 2\pi \times 0.1$ MHz. (a) Pulse shapes for STIRAP. (b) Population evolution for STIRAP. (c) Pulse shapes for STA. (d) Population evolution for STA. The Gaussian pulses are given with parameters $\Omega_0 = 2/T$, $\tau_s = 0.5T$, and $\tau_p = -0.5T$.

Fig. 2(d). It should be noted that the auxiliary pulses Ω_a and Ω_b can be ignored, since the dark-state evolution does not involve the intermediate state $|2\rangle$.

In the intuitive sequence, the population transfer goes along the adiabatic passage $|\lambda_+ \rangle$ or $|\lambda_- \rangle$, which is called the bright STIRAP. In this sequence, the mixing angle θ is initially to be $\pi/2$, and then to be zero at the end of the population transfer. The angle ϕ selects the accurate adiabatic passage corresponding to the population evolution. For simplicity, we consider the case $\Delta \neq 0$ where the angle ϕ is zero throughout the transition. In the adiabaticity condition, this implies that the population transfer will reside in the adiabatic passage $|\lambda_- \rangle$ without the undesired diabatic transitions, and the desired state transition from the initial state $|1\rangle$ to the target state $|3\rangle$ can be achieved. As the adiabaticity condition is destroyed by the pulse intensities, the population evolution in the designed passage $|\lambda_- \rangle$ may jump to the other passages $|\lambda_0\rangle$ and $|\lambda_+ \rangle$, which may induce a loss of the transfer efficiency. As the pulses shown in Fig. 3(a) violate the adiabaticity condition, the transfer efficiency is only 76.7% depicted in Fig. 3(b). When the undesired diabatic transitions are eliminated in STA by introducing the auxiliary pulses Ω_a , Ω_b , and Ω_c , the population transfer can be exactly limited in the adiabatic passage $|\lambda_- \rangle$. Therefore a complete population transfer could be achieved as Fig. 3(d) depicts.

The above two cases of counterintuitive and intuitive sequences demonstrate that STA is more efficient than STIRAP for population transfer in the same pulse shapes and intensities. In STIRAP, the population transfer could be designed under the adiabaticity condition to obtain a high transfer efficiency, but the diabatic transitions among the adiabatic passages actually exist throughout the evolution. Thus, the unavoidable fluctuations of the pulse intensities may destroy the adiabaticity condition, and cause a loss of the transfer efficiency [52]. On the other hand, in STA, the diabatic transitions are completely eliminated by the auxiliary pulses, and the transfer efficiency is more insensitive to the detunings and Rabi frequencies. These features of STIRAP and STA are depicted in Fig. 4. Here, plots of the final population ρ_{33} are shown as a function of the peak Rabi frequency Ω_0 for

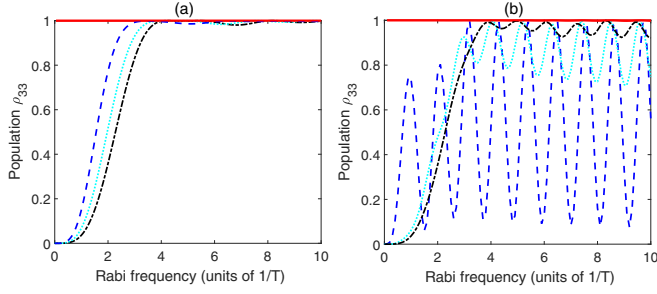


FIG. 4. Final population ρ_{33} as a function of the peak Rabi frequency Ω_0 for different detunings. (a) The dark-state evolution $|\lambda_0\rangle$. (b) The bright-state evolution $|\lambda_-\rangle$. The solid red line is for STA, and the others are for STIRAP. Dashed blue, dotted cyan, and dash-dotted black lines correspond to the detunings 0.2π , 0.8π , and 1.2π MHz.

different detunings. In STIRAP, to obtain a complete population transfer, the Rabi frequency should be sufficiently strong both in the bright and dark adiabatic passages to match the adiabaticity condition, and a large detuning needs a strong Rabi frequency. However, in STA, the complete population transfer can be sufficiently achieved beyond the adiabaticity condition, and a fast progress could be induced by the strong pulses. The final population in STA can be always kept at the high efficiency of 100%, as the Rabi frequency and detuning do not change the transfer efficiency. Therefore, we can obtain the conclusion that STA is faster than STIRAP to control the population transfer.

III. SPONTANEOUS EMISSION WITHIN A THREE-STATE SYSTEM

Considering spontaneous emission from the excited state $|2\rangle$, we use the master (Liouville) equation to describe the dynamics of the system. Generally, as the spontaneous emission is phenomenologically described, the master equation takes the following form [53,54]:

$$i\dot{\rho} = [H(t), \rho] + D, \quad (7)$$

where the matrix D is relative to the spontaneous emission,

$$D = -\frac{i}{2} \begin{pmatrix} -2\Gamma_1\rho_{22} & (\Gamma_1 + \Gamma_2)\rho_{12} & 0 \\ (\Gamma_1 + \Gamma_2)\rho_{21} & (\Gamma_1 + \Gamma_2)\rho_{22} & (\Gamma_1 + \Gamma_2)\rho_{23} \\ 0 & (\Gamma_1 + \Gamma_2)\rho_{32} & -2\Gamma_2\rho_{22} \end{pmatrix}, \quad (8)$$

with Γ_1 and Γ_3 being the decay rates of spontaneous emission from the excited state $|2\rangle$. The relative decay rate for each pair of states is depicted by the green wavy line in Fig. 1. We assume that the two decay rates are equal to simplify the treatment and introduce a dimensionless decay rate $\gamma = \Gamma T$. ρ is the density matrix in the bare state $|m\rangle$, i.e., $\rho_{mn} = \langle m|\rho|n\rangle$ ($m, n = 1, 2, 3$). Equation (7) is solved with the condition that the system is initially in the state $|1\rangle$, $\rho_{11}(-\infty) = 1$, $\rho_{mn}(-\infty) = 0$, ($m, n \neq 1$).

A unique feature for population transfer in the counterintuitive sequence is that the intermediate state $|2\rangle$ is unpopulated along the dark adiabatic passage $|\lambda_0\rangle$. In STIRAP, the pump and the Stokes pulses are usually designed under the adiabaticity condition to suppress the undesired diabatic transitions. Even though the probabilities of the diabatic transitions are

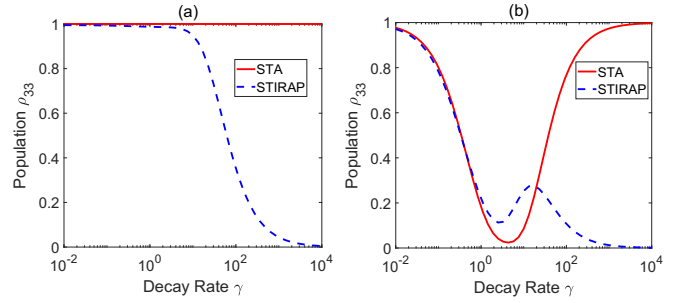


FIG. 5. Final population ρ_{33} as a function of the spontaneous emission rate γ with the detuning $\Delta = 2\pi \times 0.1$ MHz. (a) The dark-state evolution $|\lambda_0\rangle$ with the peak Rabi frequency $\Omega_0 = 6/T$. (b) The bright-state evolution $|\lambda_-\rangle$ with the peak Rabi frequency $\Omega_0 = 3.2/T$. The solid red and dashed blue lines depict the STA and STIRAP, respectively.

sufficiently small, the intermediate state $|2\rangle$ could be populated during the excitation. Therefore, the population losses may occur owing to diabatic transitions from the passage $|\lambda_0\rangle$ to the passages $|\lambda_{\pm}\rangle$. The other mechanism for population losses in STIRAP is quantum overdamping. The population remains predominantly in the initial state; the transfer to state $|3\rangle$ is suppressed at large Γ . These mechanisms for population losses via STIRAP are depicted by the dashed blue line in Fig. 5(a). When the spontaneous emission rate is sufficiently small ($\gamma \ll 1$), the diabatic transitions are still perfectly suppressed, the population evolution is approximately in the dark adiabatic passage $|\lambda_0\rangle$ and the effect of dissipation could be neglected with a high transfer efficiency of 100%. As the spontaneous emission becomes strong ($\gamma \sim 1$), the adiabaticity condition is destroyed by the spontaneous emission, the intermediate state $|2\rangle$ is obviously populated according to the diabatic transitions, and the population loss is presented. For a large decay rate ($\gamma \gg 1$), the population is held in the initial state $|1\rangle$. Different from STIRAP, STA has the property to completely eliminate the diabatic transitions; the population evolution exactly goes along the dark adiabatic passage $|\lambda_0\rangle$ with no visiting to the state $|2\rangle$. Therefore, the spontaneous emission has no contribution to the population losses, and the final population of the state $|3\rangle$ could be held in a high transfer efficiency of 100% depicted by the solid red line in Fig. 5(a).

In the intuitive sequence, the intermediate state $|2\rangle$ is notably involved in the population transfer along the bright adiabatic passage $|\lambda_-\rangle$. The population losses for the two proposals are quite equal in the weak decay rate ($\gamma \ll 1$). When the spontaneous emission becomes strong ($\gamma \sim 1$), the transfer efficiency of STIRAP seems higher than that of STA. The reason for this phenomenon is that the diabatic transitions in STIRAP induce a dark-state evolution. Population evolution initially in the adiabatic passage $|\lambda_-\rangle$ is excited to the dark adiabatic passage $|\lambda_0\rangle$ where spontaneous emission has no contribution to the population losses. When the spontaneous emission is large enough to decouple the intermediate state $|2\rangle$ ($\gamma \gg 1$), a very interesting phenomenon is presented that the adiabatic passage $|\lambda_-\rangle = \sin\theta \cos\phi|1\rangle - \sin\phi|2\rangle + \cos\theta \cos\phi|3\rangle$ is simplified as $|\lambda_-\rangle = \sin\theta|1\rangle + \cos\theta|3\rangle$. This adiabatic passage is similar to the dark adiabatic passage $|\lambda_0\rangle$, thus the population can be completely transferred to the target

state $|3\rangle$ in STA depicted in Fig. 5(b). In STIRAP, although the three-state system can degenerate to be a two-state system with the states $|1\rangle$ and $|3\rangle$, there are no auxiliary pulses to drive the two states, and the population remains in the initial state $|1\rangle$.

We should note that the pump and Stokes pulses in this section are designed in the adiabaticity condition to drive the population transfer. In the closed system with no spontaneous emission, it is clear to see that the diabatic transitions among the adiabatic states are both neglected in the two approaches, STA and STIRAP. As the spontaneous emission is introduced to the intermediate state $|2\rangle$, the system initially in an adiabatic regime may undergo a transition to a regime where adiabaticity breaks down and the diabatic transitions may occur during the population evolution [55,56]. However, as the complete population transfer in STA can be beyond the adiabaticity condition, and the diabatic transitions are completely eliminated, the population losses directly come from the intermediate state $|2\rangle$. In the weak decay region ($\gamma \ll 1$), the spontaneous emission is not strong enough to trigger the diabatic transitions; the population evolutions of the two approaches are quite similar with the same transfer efficiency depicted in Fig. 5. As the decay rate becomes strong enough to trigger the diabatic transitions ($\gamma \sim 1$), the differences are presented in STA and STIRAP. In STA, the spontaneous emission has no effect on the population transfer in the dark adiabatic passage $|\lambda_0\rangle$. The population losses are only presented in the bright adiabatic passage $|\lambda_-\rangle$ where the intermediate state $|2\rangle$ is involved. In STIRAP, owing to the diabatic transitions induced by the spontaneous emission, the transfer efficiency decreases in the dark adiabatic passage $|\lambda_0\rangle$, but seems higher in the bright adiabatic passage $|\lambda_-\rangle$. When the decay rate becomes very strong ($\gamma \gg 1$), the transfer efficiency in STIRAP is quite low; even the population remains in the initial state $|1\rangle$. However, in STA, the transfer efficiency goes back to be at a high level in the bright adiabatic passage $|\lambda_-\rangle$, and the spontaneous emission still has no effect on the dark adiabatic passage $|\lambda_0\rangle$.

IV. CONCLUSIONS

In summary, we have demonstrated that STA is superior to STIRAP for population transfer. As the auxiliary pulses

are introduced in STIRAP to drive the population transfer, the diabatic transitions among the adiabatic passages are completely eliminated. Therefore, population transfer in STA can be strictly limited in the initial designed adiabatic passage to achieve the desired target. We have shown that STA can achieve a more effective population transfer than STIRAP in the same situation both in the dark and bright adiabatic passages. The efficiency of the target state in STA is always kept on a high level of 100% in different intensities of detunings and Rabi frequencies.

Importantly, we have examined the effects of spontaneous emission from the intermediate state $|2\rangle$ on the population dynamics in a three-state system. Compared with STIRAP, the diabatic transition in STA is still suppressed, and population transfer is robust with a high efficiency against the spontaneous emission. In the counterintuitive pulse sequence, the population dynamics goes along the dark adiabatic passage $|\lambda_0\rangle$ where the intermediate state $|2\rangle$ is not involved, thus spontaneous emission has no contribution to the population losses. On the other hand, in the intuitive pulse sequence, the population dynamics goes along the bright adiabatic passage $|\lambda_-\rangle$; the population losses come from the direct dissipation from the intermediate state $|2\rangle$. A remarkable and interesting phenomenon is that the transfer efficiency may go back to remain at a high level, when the system is overdamping ($\gamma \gg 1$). We should note that quantum overdamping will completely separate the intermediate state $|2\rangle$ from the other states in STA, so the three-state system can be decoupled to be a two-state model with states $|1\rangle$ and $|3\rangle$. With the auxiliary pulses in STA, complete population transfer could be realized from the initial state $|1\rangle$ to the target state $|3\rangle$, and the spontaneous emission from the intermediate state $|2\rangle$ can be sufficiently ignored.

ACKNOWLEDGMENTS

This work was supported in part by the National Natural Science Foundation of China under Grants No. 61775214 and No. 61601433, the Natural Science Foundation of Chongqing, China under Grants No. cstc2019jcyj-msxmX0387 and No. cstc2019jcyj-zdxm0098, and the Youth Innovation Promotion Association of the Chinese Academy of Sciences.

-
- [1] D. Guéry-Odelin, A. Ruschhaupt, A. Kiely, E. Torrontegui, S. Martínez-Garaot, and J. G. Muga, *Rev. Mod. Phys.* **91**, 045001 (2019).
 - [2] A. Ruschhaupt, X. Chen, D. Alonso, and J. G. Muga, *New J. Phys.* **14**, 093040 (2012).
 - [3] Y.-C. Li and X. Chen, *Phys. Rev. A* **94**, 063411 (2016).
 - [4] E. Torrontegui, I. Lizuain, S. González-Resines, A. Tobalina, A. Ruschhaupt, R. Kosloff, and J. G. Muga, *Phys. Rev. A* **96**, 022133 (2017).
 - [5] D. Guéry-Odelin and J. G. Muga, *Phys. Rev. A* **90**, 063425 (2014).
 - [6] X. Chen, I. Lizuain, A. Ruschhaupt, D. Guéry-Odelin, and J. G. Muga, *Phys. Rev. Lett.* **105**, 123003 (2010).
 - [7] M. V. Berry, *J. Phys. A* **42**, 365030 (2009).
 - [8] X. Shi, H. Yuan, X. Mao, Y. Ma, and H. Q. Zhao, *Phys. Rev. A* **95**, 052332 (2017).
 - [9] S. Ibáñez, Xi Chen, E. Torrontegui, J. G. Muga, and A. Ruschhaupt, *Phys. Rev. Lett.* **109**, 100403 (2012).
 - [10] X. Chen and J. G. Muga, *Phys. Rev. A* **86**, 033405 (2012).
 - [11] F. Impens and D. Guéry-Odelin, *Phys. Rev. A* **96**, 043609 (2017).
 - [12] E. Torrontegui, S. Martínez-Garaot, A. Ruschhaupt, and J. G. Muga, *Phys. Rev. A* **86**, 013601 (2012).
 - [13] J. Li, K. Sun, and X. Chen, *Sci. Rep.* **6**, 38258 (2016).
 - [14] D. Sels and A. Polkovnikov, *Proc. Natl. Acad. Sci. USA* **114**, E3909 (2017).
 - [15] P. Richerme, C. Senko, J. Smith, A. Lee, S. Korenblit, and C. Monroe, *Phys. Rev. A* **88**, 012334 (2013).

- [16] X. Chen, A. Ruschhaupt, S. Schmidt, A. del Campo, D. Guéry-Odelin, and J. G. Muga, *Phys. Rev. Lett.* **104**, 063002 (2010).
- [17] R. Bowler, J. Gaebler, Y. Lin, T. R. Tan, D. Hanneke, J. D. Jost, J. P. Home, D. Leibfried, and D. J. Wineland, *Phys. Rev. Lett.* **109**, 080502 (2012).
- [18] E. Torrontegui, Xi Chen, M. Modugno, A. Ruschhaupt, D. Guéry-Odelin, and J. G. Muga, *Phys. Rev. A* **85**, 033605 (2012).
- [19] S. Martínez-Garaot, E. Torrontegui, Xi Chen, M. Modugno, D. Guéry-Odelin, S.-Y. Tseng, and J. G. Muga, *Phys. Rev. Lett.* **111**, 213001 (2013).
- [20] S. Guérin, V. Hakobyan, and H. R. Jauslin, *Phys. Rev. A* **84**, 013423 (2011).
- [21] M. Kolodrubetz, D. Sels, P. Mehta, and A. Polkovnikov, *Phys. Rep.* **697**, 1 (2017).
- [22] X. Chen, E. Torrontegui, and J. G. Muga, *Phys. Rev. A* **83**, 062116 (2011).
- [23] J.-L. Wu, X. Ji, and S. Zhang, *Sci. Rep.* **7**, 46255 (2017).
- [24] A. C. Santos, R. D. Silva, and M. S. Sarandy, *Phys. Rev. A* **93**, 012311 (2016).
- [25] Z.-T. Liang, X. Yue, Q. Lv, Y.-X. Du, W. Huang, H. Yan, and S.-L. Zhu, *Phys. Rev. A* **93**, 040305(R) (2016).
- [26] Y.-X. Du, B.-J. Liu, Q.-X. Lv, X.-D. Zhang, H. Yan, and S.-L. Zhu, *Phys. Rev. A* **96**, 012333 (2017).
- [27] D. Stefanatos, *Phys. Rev. A* **90**, 023811 (2014).
- [28] G. Della Valle, *Phys. Rev. A* **98**, 053861 (2018).
- [29] Y.-H. Kang, Y.-H. Chen, Z.-C. Shi, B.-H. Huang, J. Song, and Y. Xia, *Phys. Rev. A* **96**, 022304 (2017).
- [30] S.-H. Wu, M. Amezcua, and H. Wang, *Phys. Rev. A* **99**, 063812 (2019).
- [31] E. Torrontegui, S. T. Dawkins, M. Göb, and K. Singer, *New J. Phys.* **20**, 105001 (2018).
- [32] J. Cohn, A. Safavi-Naini, R. J. Lewis-Swan, J. G. Bohnet, M. Gärttner, K. A. Gilmore, J. E. Jordan, A. M. Rey, J. J. Bollinger, and J. K. Freericks, *New J. Phys.* **20**, 055013 (2018).
- [33] B.-J. Liu, X.-K. Song, Z.-Y. Xue, X. Wang, and M.-H. Yung, *Phys. Rev. Lett.* **123**, 100501 (2019).
- [34] H. Ribeiro and A. A. Clerk, *Phys. Rev. A* **100**, 032323 (2019).
- [35] D. Stefanatos and E. Paspalakis, *Phys. Rev. A* **99**, 022327 (2019).
- [36] X. Shi and L. F. Wei, *Laser Phys. Lett.* **12**, 015204 (2015).
- [37] M. G. Bason, M. Viteau, N. Malossi, P. Huillery, E. Arimondo, D. Ciampini, R. Fazio, V. Giovannetti, R. Mannella, and O. Morsch, *Nat. Phys.* **8**, 147 (2012).
- [38] B. B. Zhou, A. Baksic, H. Ribeiro, C. G. Yale, F. Joseph Heremans, P. C. Jerger, A. Auer, G. Burkard, A. A. Clerk, and D. D. Awschalom, *Nat. Phys.* **13**, 330 (2017).
- [39] J. Kölbl, A. Barfuss, M. S. Kasperczyk, L. Thiel, A. A. Clerk, H. Ribeiro, and P. Maletinsky, *Phys. Rev. Lett.* **122**, 090502 (2019).
- [40] Y.-X. Du, Z.-T. Liang, Y.-C. Li, X.-X. Yue, Q.-X. Lv, W. Huang, X. Chen, H. Yan, and S.-L. Zhu, *Nat. Commun.* **7**, 12479 (2016).
- [41] S. An, D. Lv, A. del Campo, and K. Kim, *Nat. Commun.* **7**, 12999 (2016).
- [42] T. Yan, B.-J. Liu, K. Xu, C. Song, S. Liu, Z. Zhang, H. Deng, Z. Yan, H. Rong, K. Huang, M.-H. Yung, Y. Chen, and D. Yu, *Phys. Rev. Lett.* **122**, 080501 (2019).
- [43] A. Vepsäläinen, S. Danilin, and G. Sorin Paraoanu, *Sci. Adv.* **5**, eaau5999 (2019).
- [44] X.-J. Lu, X. Chen, A. Ruschhaupt, D. Alonso, S. Guérin, and J. G. Muga, *Phys. Rev. A* **88**, 033406 (2013).
- [45] Y. H. Issoufa and A. Messikh, *Phys. Rev. A* **90**, 055402 (2014).
- [46] S. Ibáñez, S. Martínez-Garaot, X. Chen, E. Torrontegui, and J. G. Muga, *Phys. Rev. A* **84**, 023415 (2011).
- [47] S. Ibáñez and J. G. Muga, *Phys. Rev. A* **89**, 033403 (2014).
- [48] Q.-C. Wu, Y.-H. Chen, B.-H. Huang, Y. Xia, and J. Song, *Phys. Rev. A* **94**, 053421 (2016).
- [49] H. Li, H. Z. Shen, S. L. Wu, and X. X. Yi, *Opt. Express* **25**, 30135 (2017).
- [50] N. V. Vitanov and S. Stenholm, *Phys. Rev. A* **56**, 1463 (1997).
- [51] K. Bergmann, H. Theuer, and B. W. Shore, *Rev. Mod. Phys.* **70**, 1003 (1998).
- [52] A. A. Rangelov, N. V. Vitanov, L. P. Yatsenko, B. W. Shore, T. Halfmann, and K. Bergmann, *Phys. Rev. A* **72**, 053403 (2005).
- [53] P. A. Ivanov, N. V. Vitanov, and K. Bergmann, *Phys. Rev. A* **72**, 053412 (2005).
- [54] M. Scala, B. Militello, A. Messina, and N. V. Vitanov, *Phys. Rev. A* **83**, 012101 (2011).
- [55] M. S. Sarandy and D. A. Lidar, *Phys. Rev. A* **71**, 012331 (2005).
- [56] M. S. Sarandy and D. A. Lidar, *Phys. Rev. Lett.* **95**, 250503 (2005).